

## THE ENVISAT ASAR MISSION: A LOOK BACK AT 10 YEARS OF OPERATION

N. Miranda<sup>(1)</sup>, B. Rosich<sup>(1)</sup>, P.J. Meadows<sup>(2)</sup>, K. Haria<sup>(3)</sup>, D. Small<sup>(4)</sup>, A. Schubert<sup>(4)</sup>, M. Lavallo<sup>(5)</sup>, F. Collard<sup>(6)</sup>,  
H. Johnsen<sup>(7)</sup>, A. Monti Guarnieri<sup>(8)</sup> & D. D'Aria<sup>(9)</sup>

<sup>(1)</sup> European Space Agency, Directorate of Earth Observation Programmes,  
ESA-ESRIN, Via Galileo Galilei 00044, Frascati, Italy. Email: nuno.miranda@esa.int, betlem.rosich@esa.int

<sup>(2)</sup> BAE Systems Advanced Technology Centre, West Hanningfield Road, Chelmsford, Essex,  
CM2 8HN, United Kingdom. Email: peter.meadows@baesystems.com

<sup>(3)</sup> Telespazio VEGA UK Ltd, 350 Capability Green, Luton, Bedfordshire, LU1 3LU, United Kingdom  
Email: kajal.haria@vegaspacespace.com

<sup>(4)</sup> Remote Sensing Laboratories, Department of Geography, University of Zurich, Winterthurerstrasse 190,  
CH-8057 Zurich, Switzerland. Email: david.small@geo.uzh.ch, schubert@geo.uzh.ch

<sup>(5)</sup> Jet Propulsion Laboratory, California Institute of Technology, 4800 Oak Grove Drive,  
Pasadena, CA 91109, USA. Email: marco.lavallo@jpl.nasa.gov

<sup>(6)</sup> Ocean Data Lab, Bat. CERSAT, IFREMER, Technopôle Brest-Iroise, 29280 Plouzané, France  
Email: dr.fab@oceandatalab.com

<sup>(7)</sup> Norut Tromsø, P.O. Box 6434, Tromsø Science Park, N-9294 Tromsø, Norway  
Email: harald.johnsen@norut.no

<sup>(8)</sup> Dipartimento di Elettronica, Informazione e Bioingegneria - Politecnico di Milano, Via Ponzio, 34/5,  
20133 Milano, Italy. Email: monti@elet.polimi.it

<sup>(9)</sup> ARESYS s.r.l., Via Bistolfi 49, 20134, Milano, Italy.  
Email: davide.daria@aresys.it

### ABSTRACT

The Advanced Synthetic Aperture Radar (ASAR) on-board Envisat operated successfully for just over 10 years until the failure of Envisat in April 2012. ASAR was ESA's very first deployment of a C-band phased-array antenna, allowing extended imaging capacity in comparison to its ERS SAR predecessors. As such it operated in various acquisition modes – Image (IM), Alternating Polarisation (AP), Wide Swath (WS), Global Monitoring (GM), and Wave (WV). For IM and AP modes there was a selection of 7 swaths with swath width from 100 km to 56 km: IM was single-polarisation, while AP was dual-pol, offering a choice from HH&VV, HH&HV, or VV&VH. WS and GM modes had a total swath width of 405 km based on the combination of 5 sub-swaths. WV acquired imagedettes of 10 km by 10 km every 100 km along the satellite track.

This paper is a look back to the 10 years of ASAR operations, covering topics such as the ASAR Instrument (characteristics, acquisition modes, product tree and observation scenario), Instrument Calibration and Performance Verification (including instrument stability, internal calibration, external calibration, absolute radiometric calibration, localisation accuracy, absolute geolocation accuracy, performance verification and product calibration), ASAR specific missions (wave and polarimetric), particular ASAR events such as

antenna resets, burst synchronisation, AP swath modifications and the Envisat orbit change in October 2010.

### 1. INTRODUCTION

The main Envisat objective was to endow Europe with an enhanced Earth Observation capability from space. The Envisat mission objectives were to contribute to the Earth's environment studies including land, ocean and polar regions, to observe the atmosphere and its chemistry, to observe the ocean, to provide data for monitoring and managing the Earth's resources and to provide continuity with the ERS mission [1].

For fulfilling these, the Envisat platform was composed of 10 different payloads (see Figure 1) providing complementary, synchronised and collocated measurements as shown in Figure 2 for the specific example of the imaging instruments.

Envisat was launched on the 1st March 2002 by an Ariane 5 rocket from Europe's spaceport in Kourou for a nominal lifetime of 5 years. It ceased operation on 8th April 2012 following a communications failure. Envisat was placed in the same orbital plane as ERS-2 with 30 minutes delay sharing the same 35 day/501 orbit repeat cycle. This specific configuration allowed further strong compatibility with its predecessor. The nominal

configuration was maintained from the beginning of the mission until the orbit change in October 2010 (Section 3.7). After the orbit change, Envisat was in a 30 day/431 orbit repeat cycle.

The most popular payload on Envisat was the Advance Synthetic Aperture Radar (ASAR) instrument. ASAR contributed to the overall mission objectives by providing all-weather, night-and-day radar backscatter over land, polar regions and oceans at different resolutions and swath widths. Furthermore, ASAR being the direct continuation of the ERS SAR mission allowed ESA to provide more than 20 years of harmonised SAR data to the scientific community (see Section 6).

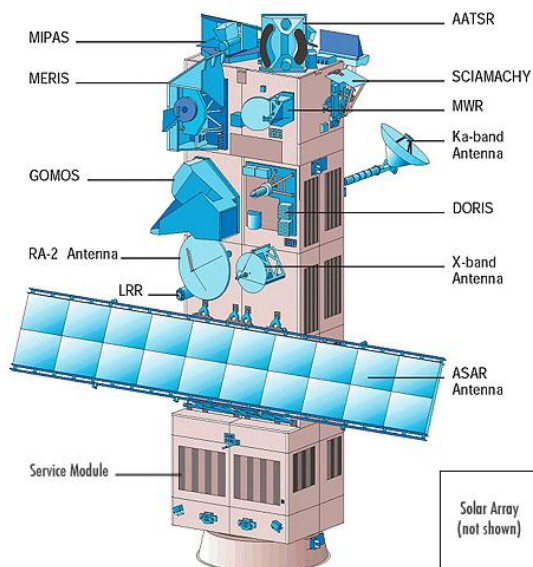


Figure 1. Envisat platform and instruments.

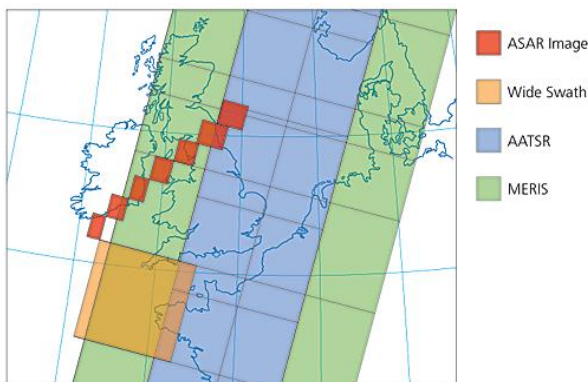


Figure 1. Example single pass swath coverage of the Envisat Imaging Instruments

## 2. ADVANCED SYNTHETIC APERTURE RADAR (ASAR) INSTRUMENT

Here the information on the ASAR instrument, acquisition modes, swath characteristics, products and observation scenario are discussed.

### 2.1. Instrument Characteristics

ASAR was a right side looking C-band Synthetic Aperture Radar working at the central frequency of 5.331 GHz with a maximum chirp bandwidth of 16 MHz. The instrument acquired data- at two different bit rates: 100 Mbps and 0.9 Mbps defining the High Bit Rate (HBR) and the Low Bit Rates (LBR) modes.

ASAR was an active phased array 10.0 x 1.3 m antenna composed of 320 Transmit/Receive Modules (TRM) organised in 20 tiles of 16 rows each. Each TRM was activated independently in gain and phase allowing a flexible electronic elevation beam steering spanning from 15° to 45° incident angle. Furthermore, each TRM consisted of two transmit channels (H&V) and one common receive channel, allowing (limited) polarimetric capability (see Section 5.2). Table 1 gives a list of ASAR characteristics.

Table 1. ASAR Characteristics

Antenna size	10m x 1.3m
Centre frequency	5.331GHz
Chirp Bandwidth	16MHz maximum
PRF	Variable (~1600Hz-2096Hz)
Incident angles	15° to 45°
Swath width	Variable 100-80 km or 400 km
Bit quantisation	5 bits
Look Direction	Right
Data rate	100Mbps or 0.9Mbps
Yaw Steering Mode	Yes

### 2.2. Acquisition Modes

ASAR was a flexible instrument in that it could be operated in 5 mutually exclusive acquisition modes. Those modes were Image Mode (IM), Alternating Polarisation (AP) Mode, the Wide Swath (WS) Mode, Global Monitoring (GM) Mode, and Wave (WV) Mode as shown in Figure 3. IM, AP, and WS were the HBR modes, while GM and WV were the LBR modes.

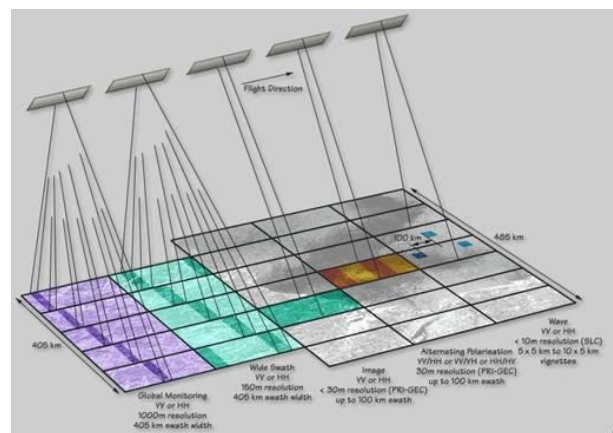


Figure 2 ASAR acquisition modes

IM was a classical stripmap mode that could be operated on one of the 7 predefined elevation beams called Image Swath (IS) from IS1 to IS7. The swath width decreased with incident angle from ~100 km to ~60 km. IM generated high resolution data-takes in single polarisation (HH or VV), each characterised beam having a different mid incident angle and coverage as indicated in Table 2. The IM/IS2/VV swath and polarisation combination was the same as for the ERS SAR, the so-called ERS-like mode.

AP shared with IM the same swath definition (IS1-IS7) but used the ScanSAR technique to provide a dual-polarisation capacity. In AP, two simultaneous images of the same area could be imaged in a co-polarisation (HH/VV) or cross-polarisation (HH/HV or VV/VH) configuration. AP generated high resolution data but with a slightly inferior radiometric resolution and a slightly larger azimuth spatial resolution in comparison to IM.

WS and GM were classical ScanSAR modes composed of 5 Sub-Swaths (SS) from SS1 to SS5 which overlapped with some of the stripmap swaths. Indeed, the beams SS2-SS5 were strictly identical to IS3-IS6. Both WS and GM provided a swath extent of 400km. WS was a relatively high resolution mode providing ~120 m spatial geometric resolution data, while GM was intended for global acquisition at the cost of a reduced spatial resolution of ~1 km. Both WS and GM were single polarisation modes using either HH or VV.

Table 2: ASAR Swath Characteristics.

Swath	Width [km]	Ground position from nadir [km]	Overlap [km]	Mid Incident angle [°]
IS1	105.1	189	N/A	18.86
SS1	134.1		N/A	
IS2	105.0	244	49.8	22.84
IS3_SS2	83.3	341	8.0	28.72
IS4_SS3	89.7	421	7.6	33.65
IS5_SS4	65.6	497	9.3	37.63
IS6_SS5	72.2	557	5.4	41.02
IS7	57.7	623	5.6	43.98

IM, AP, WS and GM were modes mainly intended to acquire over land, coast and polar regions, while WV was dedicated to the monitoring of the open oceans. WV acquired vignettes of 10x10 km every 100 km along the satellite track. The vignettes (also called imagettes) could be acquired over one of the 7 predefined different IS1-IS7 swaths in either VV or HH polarisation.

GM and WV modes aimed to acquire global radar measurements over the world at the cost of a limited coverage (WV) or a limited resolution (GM).

This instrument flexibility added complexity at the calibration level, as the large number of different combination of elevation beams and polarisations required calibration (Section 4). In addition to the 5 imaging modes, ASAR could acquire in two calibration modes: External Calibration (EC) [2] mode and Module Stepping Mode (MSM). The first was used to characterise the passive part of the antenna, the calibration loop and the mechanical mispointing. The second was used to derive precise status and behaviour of the 320 TRMs in amplitude and phase [3].

### 2.3. ASAR Product Tree

From the 5 different possible acquisition modes, a full product family was defined to serve a wide range of applications and users. The ASAR product tree comprises the following classes:

- RAW products: unprocessed and un-calibrated SAR products.
- Single Look Complex (SLC) products. These are considered to be the basic products as they preserve the phase of the radar signal. These products maintain the instrument geometry (slant-range) and natural pixel sampling.
- Precision Image (PRI) products. These are detected and lightly spatially averaged to obtain square pixels and projected into the ground range plane while maintaining path orientation (azimuth, range).
- Geocoded Ellipsoid Corrected (GEC) products: similar to PRI products except projected on to a map geometry (easting, northing) using the WGS84 reference ellipsoid.
- Medium Resolution (MR) products: detected and strongly averaged to obtain square pixels and projected into the ground range plane while maintaining path orientation.

For the particular case of the WV mode data, the product definition has been oriented towards oceanographic applications leading to very specific products:

- Imagettes (WVI): a small SLC SAR image (10 km by 10 km) acquired at regular intervals of 100 km along-track and cross spectra generated from imagettes.
- Imagette Cross Spectra (WVS): as for WVI but just the cross spectra.
- Ocean Wave Spectra (WVW): the Level 2 version of the WVI product.

The full product family is listed in Table 3 using the classical mnemonics to distinguish them.

Table 3: ASAR Product Family

level	class	Acquisition Modes				
		IM	AP	WS	GM	WV
L0	RAW	L0	L0	L0	L0	L0
L1	SLC	IMS	APS	WSS	-	WVI
	PRI	IMP	APP	-	-	-
	GEC	IMG	APG	-	-	-
	MR	IMM	APM	WSM	GM1	-
	Spectra	-	-	-	-	WVS
L2	Ocean Spectra	-	-	-	-	WVW

All the ASAR products are generated by the ESA standard processing facility PF-ASAR which is installed at all the Envisat Ground Stations and Processing Centres (PACs). This ensures product consistency independent of the processing centre.

Several processor upgrades took place since the launch of Envisat in order to cope with instrument setting changes and to improve the product quality. For example, in 2005, ESA introduced the new Wide Swath SLC (WSS) product to expedite ScanSAR interferometry and the derivation of wave fields from ScanSAR data.

Further information on ASAR products can be found in the ASAR product specification document [4].

## 2.4. ASAR Observation Scenario

ASAR was functioning very close to its maximum capacity. In the absence of any user request the instrument was tasked according to a predefined Background Mission (BM) for the LBR modes and a Background Regional Mission (BRM) planning for the HBR modes. The aim of this default planning was to build a consistent data archive over areas with the mode most often requested by the user community, fully exploiting the satellite resources.

### 2.4.1. ASAR Background Mission (BM)

LBR modes (WV & GM) were operated according to user demand. In the absence of user requests, GM/HH was used over land and polar areas and WV over oceans, when the instrument was not operated in HR modes. In order to provide continuity with the ERS Wave mission, the default WV configuration was IS2/VV for ASAR. This configuration was kept from the beginning of the mission except for dedicated short calibration/validation campaigns in IS4/HH.

### 2.4.2. ASAR Background Regional Mission (BRM)

For HR modes, the instrument was operated according

to user demands. In cases of no specific demand, ASAR operated according to a predefined Background Regional Mission (BRM) which defined the default acquisition plan. In general, WS/VV was used over coastal areas while IM and more precisely IS2/VV (ERS-like) were set where continuity with ERS was requested. These default modes were superseded by user requests unless they fell within specific areas where further restrictions were applied.

## 3. ASAR Mission Events

There were several major events that occurred during the Envisat mission that had an impact on ASAR data and products. These events are discussed below.

### 3.1. ASAR Data Subsystem Redundancy Switch (May 2003)

First signs of an on-board anomaly were found with the quality of ASAR data just after launch although no problems were detected from the instrument telemetry. Then a failure was found on the Q-branch of the on-board transmitter. ASAR was switched down on 14th May 2003 to change the data subsystem (DSS) from side A to side B. Following the switch to DSS-B redundancy ASAR operations resumed on 2nd June 2003 with nominal data quality [5].

The impact of using the DSS-A and the resumption of nominal operations with DSS-B can be seen through the gain of the MSM data acquired before and after the redundancy switch (MSM data measures the gain and phase of all 320 transmit/receive modules). This is illustrated in Figure 4 (transmit H polarisation gain only) which shows the maximum, mean and minimum gain from the active ASAR TRMs from launch to the end of 2003. The gains are relative to the start of the mission. This shows that in general the MSM gains were higher than the pre-launch value before the switch and close to the pre-launch values afterwards.

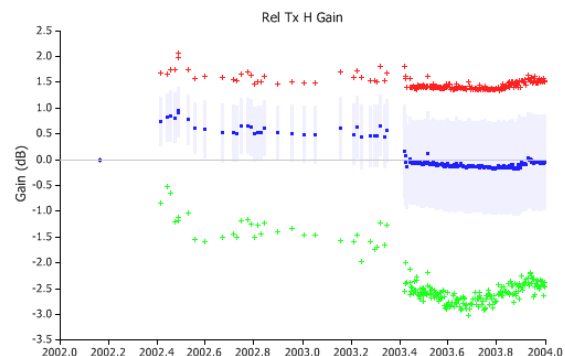


Figure 4. ASAR TRM Antenna Gain before and after the ASAR Data Subsystem Redundancy Switch (Tx H Gain only) G=Minimum, B=Mean, R=Maximum.

### 3.2. ASAR Antenna Reset#1 (September 2005)

The stability of the ASAR antenna was assessed by the behaviour of the antenna TRMs. These were monitored daily using the MSM products which was a dedicated ASAR calibration mode. In the MSM products, the 320 independent TRMs were sampled in gain and phase in less than one second.

A drift in the gain and phase of most TRMs was seen from the start of the mission. Due to the accumulated gain and phase drift for a large percentage of the TRMs, the first of two antenna resets was performed on 14th and 16th September 2005 in order to correct, as far as possible, the TRM drift.

Figure 5 shows the maximum, mean and minimum gain and phase from the active ASAR TRMs (Tx H only) from just before to just after the first antenna reset (for the mean gain or phase one standard deviation above and below the mean is also shown). The gain and phases are relative to the start of the mission. This shows also the improvement in all gains and phases after the reset.



Figure 5(a). ASAR TRM Antenna Gain before and after the ASAR Antenna Reset#1 (Tx H Gain only)

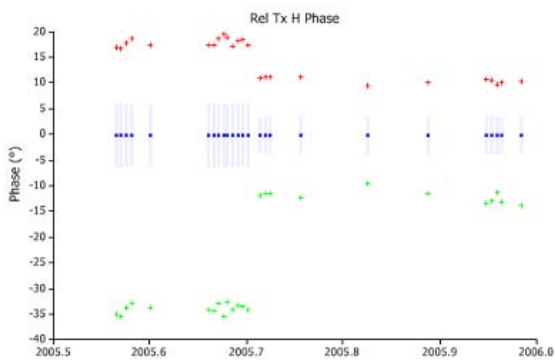


Figure 5(b). ASAR TRM Antenna Phase before and after the ASAR Antenna Reset#1 (Tx H Gain only)

### 3.3. ASAR Wide-Swath Burst Synchronisation (September 2006)

To perform interferometry with ASAR WS imagery, it is necessary for there to be an overlap in the bursts from the pair of products in each of the sub-swaths. If there is no overlap in the bursts (in azimuth), then it will not be possible to generate an interferogram (since there will be no correlation between the pair of products as the same point on the ground would be imaged by a different part of the azimuth beam). The acquisition start times for ASAR WSM imagery were altered in September 2006 so it started at discrete points around the orbit to maximise the chances of burst overlap between pairs of products – see Figure 6.

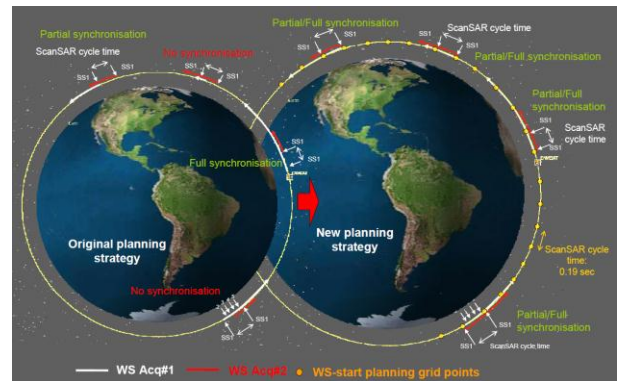


Figure 6. Illustration of the original and revised ASAR WS planning strategy (taken from [6]).

The revised planning strategy became operational from 17th September 2006 (orbit 23783). Analysis of the burst synchronisation percentage before and after the optimisation [6], the probability of burst overlaps better than 70% almost doubled. In particular, the probability of a greater than 50% burst overlap increased from 50% to 90% while the probability of a greater than 80% burst overlap increased from 30% to 50%.

### 3.4. Re-Calibration of IM and AP Modes (January 2007)

A radiometric re-calibration of ASAR IM and AP modes was performed in December 2006 and January 2007. Following the successful re-deployment of three ASAR transponders from The Netherlands to Kalimantan (Indonesia), Resolute (Canada) and Ottawa (Canada) since mid-2006 [7], many more transponder measurements had been obtained. This made it possible to perform a detailed analysis of the ASAR transponder relative radar cross-section (RCS) as a function of product type, swath and polarisation. This analysis showed the necessity of performing a re-calibration via the generation of revised calibration constants. The product types affected by this re-calibration were IMP, IMG, IMS and IMM together with APP, APG, APS and APM. The re-calibration was applicable for all products acquired since the start of the ASAR mission.

Table 4 gives the difference between the old and new calibration constants,  $\Delta K$ , where  $K_{new} = K_{old} + \Delta K$  (changes other than 0dB are marked in red). The consequence of the new calibration constants on distributed and point target radar cross-section measurements is  $RCS_{new} = RCS_{old} - \Delta K$ .

Table 4(a) ASAR  $\Delta K$  (dB) for IM products

Product	Pol	IS1	IS2	IS3	IS4	IS5	IS6	IS7
IMP	VV	0.46	0.30	0.51	0.41	0.27	0.75	0.73
IMP	HH	0.00	0.00	-0.43	0.00	0.00	0.00	-0.34
IMG	VV	0.68	0.32	0.51	0.40	0.00	0.44	0.78
IMG	HH	0.28	0.00	-0.64	0.00	0.00	0.00	-0.80
IMS	VV	0.00	-0.35	0.48	-0.24	0.00	0.00	0.65
IMS	HH	-0.43	-1.14	-0.86	-0.70	0.00	-0.64	-0.79
IMM	VV	1.13	0.64	0.69	0.57	0.95	0.00	0.98
IMM	HH	1.06	0.00	0.00	-0.36	1.07	1.03	0.00

Table 4(b) ASAR  $\Delta K$  (dB) for AP products

Prod	Pol	IS1	IS2	IS3	IS4	IS5	IS6	IS7
APP	VV/ VH	0.00	-0.62	-0.91	-0.42	-0.62	-0.44	-1.02
APP	HH/ HV	0.00	-1.08	-1.12	-0.48	-0.85	-1.02	-1.53
APG	VV/ VH	0.00	-0.63	-1.07	-0.37	-0.52	-0.30	-1.09
APG	HH/ HV	0.00	-1.01	-1.13	-0.49	-0.94	-1.29	-1.56
APS	VV/ VH	0.00	-0.39	-1.34	0.00	0.00	-0.63	-0.62
APS	HH/ HV	0.00	-0.90	-1.63	0.00	-0.83	-1.66	-1.30
APM	VV/ VH	-0.26	-0.84	-0.59	-0.29	0.00	0.48	0.70
APM	HH/ HV	0.00	-0.52	-0.39	0.28	0.62	1.03	0.78

After the re-calibration activity, updated ASAR external calibration (ASA\_XCA\_AX) auxiliary files were generated on 30th January 2007 and disseminated to the processing centres in order for the new K values to be included in all subsequently processed IM and AP products.

No further calibration constant updates were required for the rest of the ASAR mission.

### 3.5. ASAR AP Swath Modifications (May 2009)

Changes were made at the end of May 2009 to the Envisat ASAR AP swaths characteristics. These were made to avoid unplanned shut-downs of the ASAR instrument that had occurred since launch when acquiring AP data. Unplanned shut-downs of the ASAR

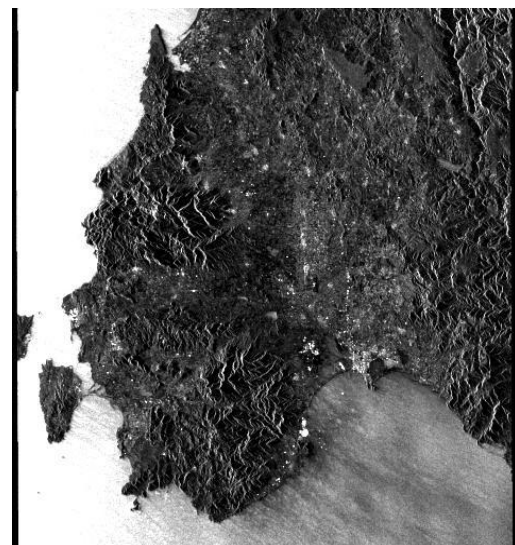
were undesirable due to their impact on the possible degradation of the instrument hardware. The number of AP acquisitions was reduced significantly in early 2007 while the usage of IS5 was suspended at the end of 2006, both to reduce the occurrence of these unplanned shut-downs [8]. A user note on this topic was issued in June 2009 [9].

This problem was caused by timing problem (between the transmit pulse and the receive window) - the solution was to change the swath width - for swaths IS2 to IS7 the near range incident angles were increased while the far range incident angles remained the same. The consequence of these changes was a reduced swath width and reduced overlap between the swaths. There were no changes for swath IS1. Table 5 shows in red the incident angles and the swath widths for the AP IS1 to IS7 swaths before and after the change on 29th May 2009 (orbit 37876).

Table 5. Old and New AP Swath Characteristics.

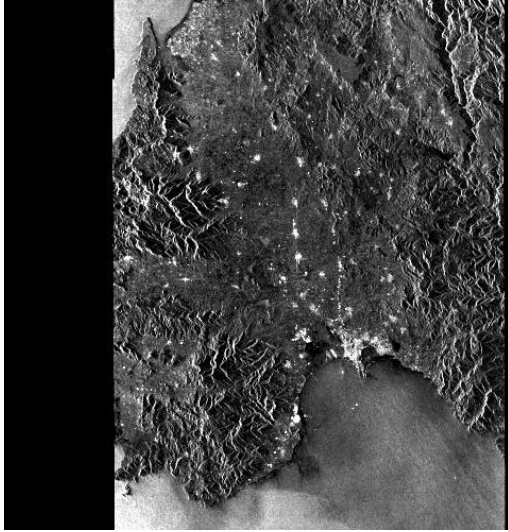
Swath	Range of Incident Angles [°]		Swath Width (ground-range) [km]	
	Old	New	Old	New
IS1	14.36 - 22.32	14.36 - 22.32	106.3	106.3
IS2	18.68 - 26.22	20.30 - 26.22	105.3	83.4
IS3	25.78 - 31.27	26.73 - 31.27	83.1	69.2
IS4	30.89 - 36.20	31.28 - 36.20	87.5	81.3
IS5	35.68 - 39.35	36.81 - 39.35	65.4	45.6
IS6	39.02 - 42.76	39.61 - 42.76	71.7	60.9
IS7	42.48 - 45.27	43.30 - 45.27	57.4	40.8

An example of the impact of the reduced AP IS2 swath is shown in Figure 6 for the same orbit track before and after the swath modification. The two images shown were acquired one repeat period apart. The reduced coverage is at near range (left of image).



27th April 2009 at 21:10 UT (orbit 37429)

Figure 6(a). Pre-AP swath modification IS2 swath



1st June 2009 at 21:10 UT (orbit 37930)

Figure 6(b). Post-AP swath modification IS2 swath

### 3.6. ASAR Antenna Reset#2 (March 2010)

The decision to perform a second ASAR antenna reset activity was based on the TRM gain and phase drifts that had occurred over the previous 4+ years.

New TRM configuration tables were uploaded on-board Envisat on the 11th March 2010 during orbits 41974-41976. Imagery acquired after the upload did not show any unexpected problems (other than the expected changes to the elevation antenna patterns). However problems were found with some of the MSM measurements. For gain, there were improvements but in Rx phase there was a problem with the 1st (top) and 17th (middle) rows. It was decided to perform a gain and phase refinement through the generation of a few new configuration files (as a similar refinement was performed in September 2005). These new configuration files were uploaded on 17th March 2010.

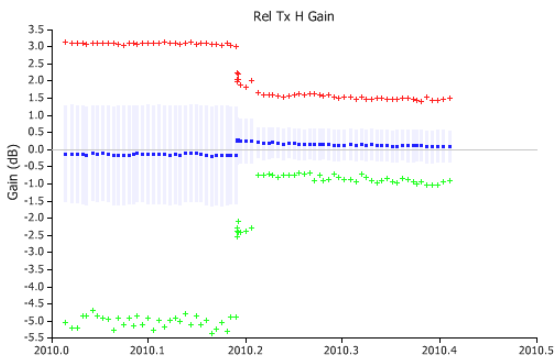


Figure 7(a). ASAR TRM Antenna Gain before and after the ASAR Antenna Reset#2 (Tx H Gain only)

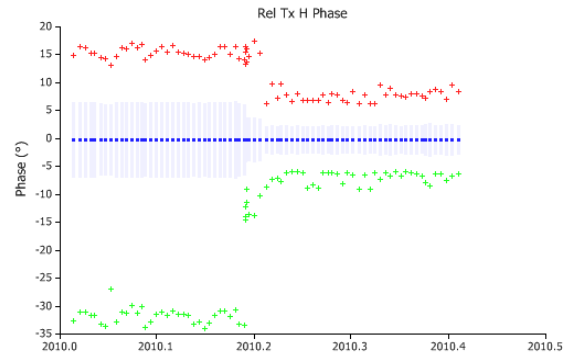


Figure 7(b). ASAR TRM Antenna Phase before and after the ASAR Antenna Reset#2 (Tx H Gain only)

### 3.7. Envisat Orbit Change (October 2010)

Envisat completed its originally foreseen mission length in March 2007. Given the excellent performance of the satellite and the interest in the science data, the mission was extended up to the end of 2010, with a further extension beyond 2010 having been assessed [10]. Because the driving constraint for that extension was the fuel availability for orbit maintenance manoeuvres, extending the Envisat mission beyond 2010 implied changes in the orbit control strategy. This would have an impact on the operations of the spacecraft and the payloads [11], on the science data [12] and on the mission. In addition, at the end of the nominal mission, the 35/501 operational orbit would have to be cleared and the satellite placed at a lower altitude, to ensure that it will not interfere with current or future missions requiring the use of this Earth Observation orbit.

The main aspects of the scenario chosen consisted of: (i) lowering the orbit by about 17.4 km, (ii) changing the repeat cycle to 30days/431 orbits and replacing altitude and inclination control by altitude control alone. These three aspects would allow significant reductions in fuel consumption and thus potentially extended the mission for 3-4 more years. The Envisat orbital configuration before and after the orbit change is shown in Figure 8.

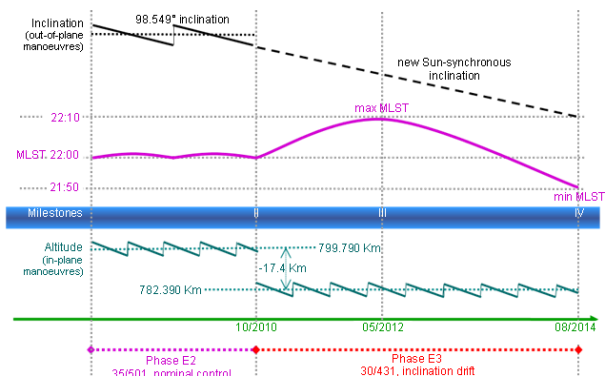


Figure 8. Envisat Orbit Change Characteristics.

The orbit lowering necessarily led to changes at the instrument level to maintain product quality. In order to limit the effort in terms of instrument re-calibration (particularly elevation antenna patterns), it was decided to keep the current beam and look angle and to redefine the swath parameters accordingly. Table 6 lists the main swath parameters for IM/AP and WS after the orbit change. Along with these characteristics, new swath parameters were derived, such as pulse repetition frequency (PRF), sampling window start time (SWST), transmit pulse length and sampling window length (SWL). These parameters were either uploaded on-board Envisat or included in new auxiliary files.

Table 6: Revised ASAR swath Characteristics

Swath	Width [km]	Overlap [km]	Mid Incident angle [°]
IS1	102.8	N/A	18.81
SS1	131.1	N/A	26.55
IS2	102.6		22.78
IS3_SS2	81.4		28.64
IS4_SS3	87.6		33.56
IS5_SS4	64.0		37.52
IS6_SS5	70.4		40.90
IS7	56.2		43.85
AP1	=IS1	N/A	
AP2	96.2	42.2	
AP3	59.8	-13.8	
AP4	64.9	-11.8	
AP5	45.0	-9.9	
AP6	52.3	-13.2	
AP7	40.2	-13.6	

Following the on-board instrument updates on 22nd October 2010, the impact on the ASAR products was assessed [12] at different levels: radiometry, geometry, and quality in general. The classical Impulse Response Function (IRF) characteristics remained unchanged or not significantly altered. The product radiometric and geometric characteristics were maintained, while the instrument sensitivity was slightly improved due to a reduced slant range distance and hence a better Signal to Noise Ratio (SNR).

The potential impact on the SAR applications was also assessed. Due to the relatively small change in altitude, most of the products would continue to suit the current land, ice, sea-ice or ocean applications, apart from Interferometric SAR (InSAR). In the case of InSAR, it was not possible to (i) systematically obtain pairs of images from before and after the orbit change and (ii) obtain pairs of images many repeat cycles apart due to the drifting orbit after the orbit change. This did, however, depend on latitude and pass type: there were optimal interferometric baselines at 38°N (descending passes) and 38°S (ascending passes). For these latitudes and pass types, it was possible to generate interferograms from data acquired several repeat periods

apart. For locations further way from these latitudes, the orbit baselines would be such that it would become progressively more difficult to generate interferograms from data acquired more than a few repeat periods apart. This is illustrated in Figure 9 which shows the baseline difference between two consecutive repeat periods as a function of cycles after the orbit change and for various northern hemisphere latitudes.

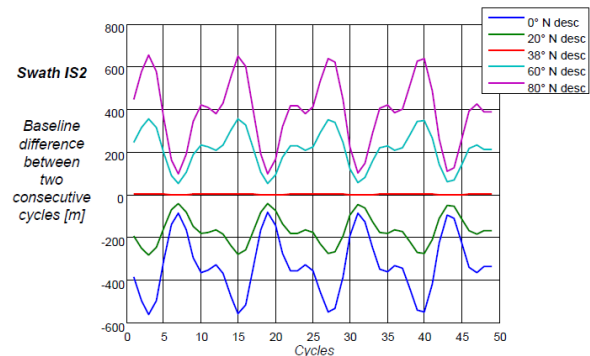


Figure 9. Baseline impact after the orbit change.

### 3.8. Antenna TRM Failures

The success of the ASAR antenna depended on there being a limited number of TRM failures during the mission (having a large number of failures would lead to significant degradation of the antenna pattern shapes). There were a total of 26 transmit horizontal polarisation failures, 20 transmit vertical polarisation failures, 8 receive horizontal polarisation failures and 8 receive vertical polarisation failures. The distribution of failures by date is shown in Table 7.

Table 7. TRM Failures by Date

Year	Number of Failures	Year	Number of Failures
2002	4	2008	2
2003	4	2009	6
2004	3	2010	2
2005	2	2011	5
2006	0	2012	0
2007	6		

Details of the individual TRM failures are:

- TRM-01 to 04 in tile C1: failed to transmit in H & V polarisation since May 2002.
- TRM-01 to 04 in tile D2: failed to transmit and receive in H & V polarisation since 18th February 2003.
- TRM-14 in tile B2: failed to transmit in H polarisation since 12th April 2004.
- TRM-15 in tile A1: failed to transmit in V polarisation since 17th May 2004.
- TRM-06 in tile A1: failed to transmit in V polarisation since 17th November 2004.



- TRM-12 in tile C4: failed to transmit in H polarisation since 16th January 2005.
- TRM-02 in tile D3: failed to transmit in V polarisation since 20th November 2005.
- TRM-03 in tile A3: failed to transmit in H polarisation since 28th January 2007.
- TRM-01-02-03-04 in tile B3: failed to transmit and receive in H & V polarisation since 2nd February 2007.
- TRM-02 in tile B1: failed to transmit in H polarisation since 6th May 2007.
- TRM-08 in tile E4: failed to transmit in H polarisation since 20th July 2008.
- TRM-05 in tile E4: failed to transmit in V polarisation since 22nd October 2008.
- TRM-10 in tile E4: failed to transmit in H polarisation since 1st January 2009.
- TRM-04 in tile D4: failed to transmit in V polarisation since 5th January 2009.
- TRM-07 in tile D2: failed to transmit in H polarisation since 7th July 2009.
- TRM-01 in tile A2: failed to transmit in H polarisation since 15th September 2009.
- TRM-05 in tile D2: failed to transmit in H polarisation since 6th October 2009.
- TRM-16 in tile E4: failed to transmit in V polarisation since 8th December 2009.
- TRM-8 in tile B4: failed to transmit in H polarisation since 26th June 2010.
- TRM-15 in tile C2: failed to transmit in H polarisation since 16th October 2010.
- TRM-14 in tile D2: failed to transmit in V polarisation since 10th March 2011.
- TRM-9 in tile B1: failed to transmit in H polarisation since 26th April 2011.
- TRM-12 in tile A1: failed to transmit in H polarisation since 19th May 2011.
- TRM-04 in tile B1: failed to transmit in H polarisation since 6th June 2011.
- TRM-08 in tile B3: failed to transmit in V polarisation since 13th September 2011.

#### 4. INSTRUMENT CALIBRATION AND PERFORMANCE VERIFICATION

The ASAR calibration and performance verification strategy was based on the well-established methodology developed for ERS. It was based on repetitive measurements over well characterised natural or man-made targets. The ASAR calibration plan relied on the Amazon rain forest for characterisation of the elevation antenna beam patterns and on extensive use of four specially developed precision transponders [13]. Transponders having a stable and known Radar Cross-Section (RCS) were used for calibration and

performance verification through analysis of their IRF. During and following the Envisat commissioning phase, four ESA transponders were deployed in various locations around The Netherlands (Aalsmeer, Swifterbant, Edam and Zwolle). In order to avoid conflicts with user requests, the calibration data requests (of higher priority) were progressively reduced to give higher priority to users. In order to satisfy the calibration needs, it was decided to move three of the transponders to different locations [7]. Thus the locations of the four transponders for the latter half of the ASAR mission were:

- TR1: stayed in Edam, The Netherlands
- TR2: moved to Resolute Bay, Nunavut in northern Canada (located close to a Radarsat transponder)
- TR3: moved to Ottawa, Canada (located close to a Radarsat transponder)
- TR4: moved to Balikpapan, Borneo in Indonesia (located at a similar latitude to the Amazon rainforest).

#### 4.1. Instrument Stability

In-flight, the instrument stability was generally measured at medium and long term levels.

Medium term checks consisted of measuring the variations of transmit and receive characteristics during an acquisition. This was done by checking the amplitude and phase of a set of internal calibration pulses and of the reconstructed chirp replica. The chirp replica was reconstructed from the internal calibration pulses; its power was later used in the ground processor for normalisation within a data-take. Figure 10 shows the stability of the replica pulse power (hence the internal calibration) within long WS data-takes acquired in 2007. It can be seen that the replica chirp variation slightly increased with data take length but largely remained below 0.1dB with an average value  $\sim 0.04$ dB. This was a good indicator of the instrument's high radiometric stability [14][15].

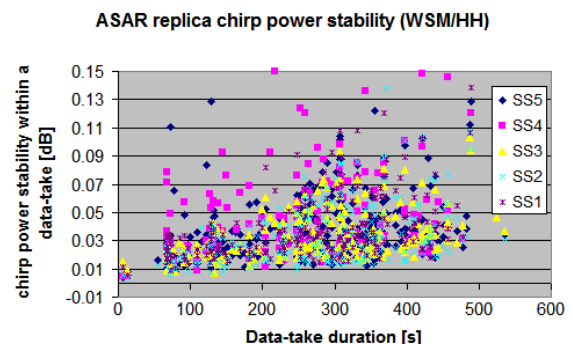


Figure 10. ASAR chirp power stability over WS data-takes acquired in April 2007.

Over a longer term, the instrument stability was mainly driven by the behaviour of the antenna TRMs. These were monitored daily using MSM products, which along with internal calibration data, indicated when and for which module a TRM failure had occurred.

Figure 11 shows the evolution of the gain and phase by showing the maximum, mean and minimum gain or phase from the active ASAR Transmit/Receive Modules (TRMs) as a function of date (for the mean gain or phase one standard deviation above and below the mean is also shown). The gains and phases are relative to the start of the mission.

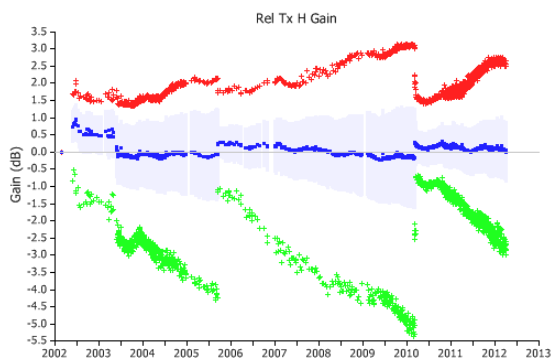


Figure 11(a). Evolution of ASAR TRM Antenna Gain during the ASAR mission (Tx H Gain only)

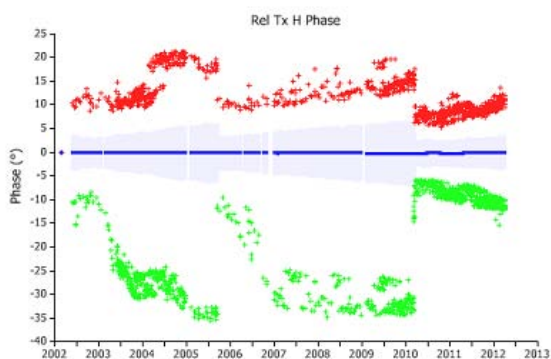


Figure 11(b). Evolution of ASAR TRM Antenna Phase during the ASAR mission (Tx H Gain only)

The impact of the ASAR DSS Redundancy Switch and the two antenna resets (Sections 3.1, 3.2 and 3.6) are clearly evident through changes in the TRM gain and phases. The regular updates of the elevation antenna patterns were effective in compensating the radiation pattern changes (Section 4.3).

#### 4.2. Doppler Centroid Monitoring

A parameter that was monitored during the ASAR mission was the Doppler centroid frequency. This parameter was extracted from ASAR products on a daily basis and it was used to monitor the attitude

stability of Envisat using WV products over ocean and GM products over land.

An example of the variation in Doppler centroid around the orbit on 5th/6th July 2010 is shown in Figure 12, where the data points away from the predicted and fitted curves were due to an out-of-plane orbit manoeuvre. Doppler centroid monitoring was useful to detect attitude anomalies that could have an impact on ASAR product quality.

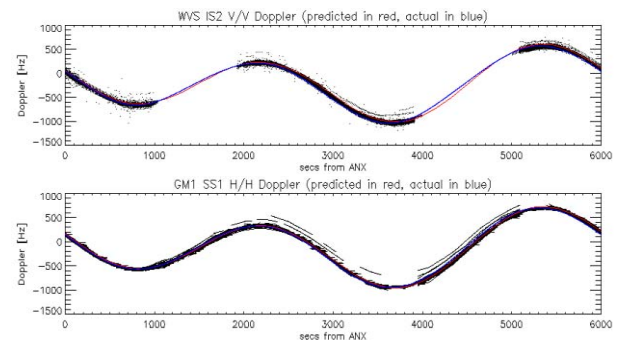


Figure 12. Doppler centroid around orbit variations on 5th/6th July 2010 during an out-of-orbit manoeuvre.

#### 4.3. Elevation Antenna Pattern Assessment

The ASAR elevation antenna patterns (EAPs) for all acquisition modes and swaths were continually measured throughout the lifetime of Envisat using suitable homogeneous regions within the Amazon rainforest.

This activity was required to monitor changes to the shape of the elevation antenna pattern caused by the failure of transmit/receive modules (Section 3.8), and to check the impact of the two antenna resets (Sections 3.2 and 3.6) and the aging of the antenna.

Updates to the elevation antenna patterns were made if there had been a change of 0.2dB or more since the previous EAP assessment (usually every 6 months). These updated EAPs were made available for use with the ESA PF-ASAR SAR processor and users via updated ASA\_XCA\_AX auxiliary files.

Figure 13 shows the EAP at the start and end of the ASAR mission for a selection of swaths: IS2 (HH and VV polarisation), IS4 (HH) and IS7 (HH). These changes were typical for all swaths and polarisations: the largest changes tended to occur in the lower incident angle swath. For all swaths there were no obvious differences in EAP changes between polarisations (including HV and VH).

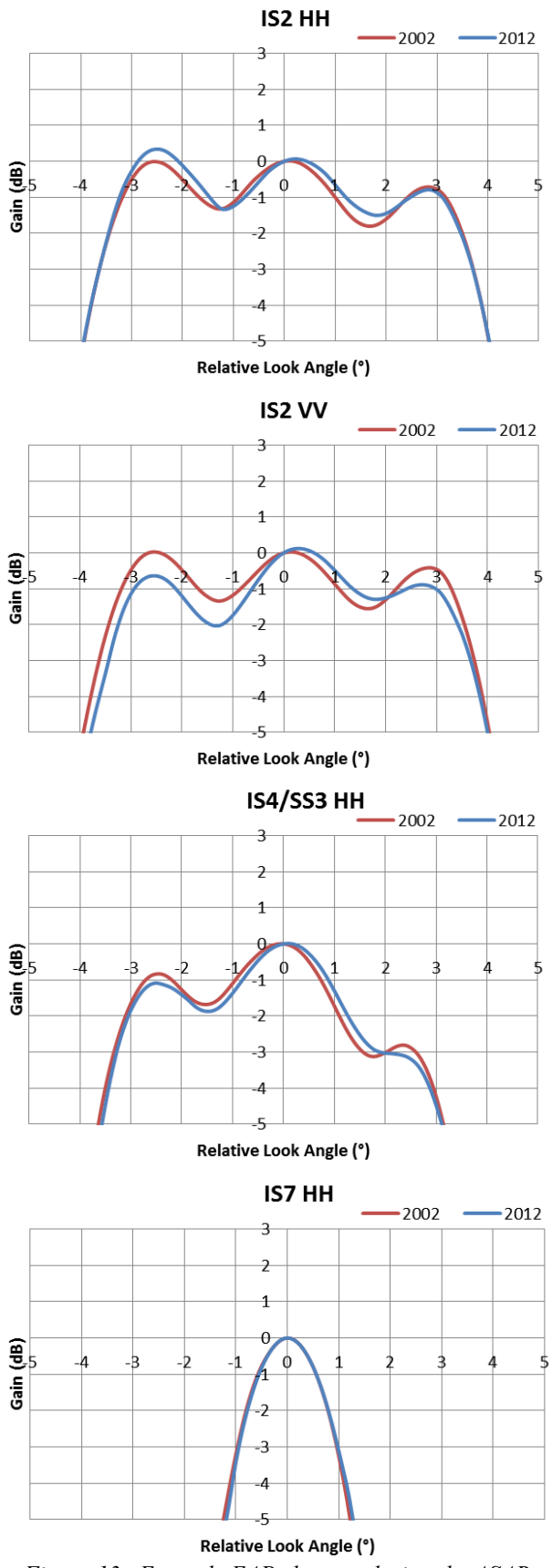


Figure 13. Example EAP changes during the ASAR mission.

#### 4.4. Radiometric Calibration

The purpose of radiometric calibration is to allow the transformation of the signal magnitude into physical units. The radar physical unit is the Radar Cross-Section RCS (or sigma expressed in dBm<sup>2</sup>) for point targets, or the Normalised RCS (NRCS) or sigma nought (RCS normalised per unit illuminated area to dB) for distributed targets with a characterised level of accuracy and stability.

The external calibration is typically subdivided into two main activities: *absolute* and *relative* radiometric calibration.

##### 4.4.1. Absolute Radiometric Calibration

Absolute radiometric calibration was achieved in the same way as for ERS by determining an absolute calibration factor (K) used to transform the pixel magnitude into physical units (RCS or NRCS). The absolute calibration factor was derived using man-made targets of known RCS.

It is preferable to use active radar calibrators (i.e. transponders) as opposed to passive ones (i.e. corner reflectors), as the ratio of signal to clutter determines the accuracy to which the calibration can be made. The RCS of the ASAR transponders themselves were (per design) within  $\pm 0.13$ dB and stable to 0.08dB, making them the targets of choice for both performance assessment and absolute calibration determination.

Table 8 lists the ASAR transponder relative RCS measurements (i.e. relative to the nominal transponder RCS) for all transponder measurements over the ASAR mission lifetime. It can be seen that the relative RCS measurements were small and consistent across the product type and swath. In terms of radiometric accuracy and stability, if considering all the ASAR transponders, the mean RCS was  $-0.21 \pm 0.58$ dB for IMP products and  $-0.13 \pm 0.52$ dB for APP products. However when considering only the reference transponders (deployed in The Netherlands) the mean RCS was  $0.04 \pm 0.40$ dB for IMP products and  $0.03 \pm 0.47$ dB from APP products, very close to the transponder specifications.

Table 8. Relative RCS measures over transponders per product type and swath.

Product type	Relative RCS [dB]							
	All Swaths	IS1	IS2	IS3	IS4	IS5	IS6	IS7
IMP	$-0.21 \pm 0.58$	-0.13	-0.22	-0.54	-0.43	-0.01	-0.01	-0.18
IMG	$-0.16 \pm 0.63$	-0.33	-0.24	-0.44	-0.43	0.17	0.12	0.00
IMS	$-0.17 \pm 0.59$	-0.31	-0.09	-0.54	-0.41	-0.04	0.10	-0.05
IMM	$-0.06 \pm 1.44$							
APP	$-0.13 \pm 0.52$	-0.53	-0.30	-0.10	-0.22	-0.03	0.32	-0.20
APG	$-0.12 \pm 0.58$	-0.52	-0.32	-0.03	-0.30	-0.14	0.42	-0.18
APS	$-0.18 \pm 0.55$	-0.39	-0.43	-0.11	-0.47	-0.15	0.23	-0.16
APM	$-0.26 \pm 0.79$							
WSM	$0.89 \pm 1.38$							

Figure 14 shows the relative RCS for the Edam transponder in The Netherlands as a function of date and polarisation as measured using IMP products.

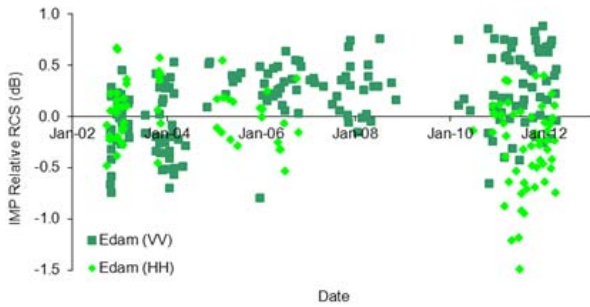


Figure 14. Edam transponder relative RCS.

#### 4.4.2. Relative Radiometric Calibration

The absolute calibration allows global correction of the image radiometry but does not allow correction for range and azimuth radiometric fluctuations in order to obtain a constant gain across the whole SAR image. This is the role of the relative calibration.

In the case of ASAR, this mainly consisted of estimating the EAP in order to remove it later during the SAR processing, or as a post-processing step. The EAP was assessed by acquiring data over the uniform Amazon Rain Forest. The EAP was regularly assessed in all the beams and polarisations and updates were made when peak-to-peak residuals of  $>0.2\text{dB}$  were seen.

Many EAP patterns were made: the full list can be found in the ASAR cyclic reports available to users [16]. In the same manner as the calibration constant, the different EAP used operationally in the ground segment are stored in Auxiliary Data Files (ADF) accessible to the users [17].

#### 4.5. Localisation Accuracy

The ASAR introduced unprecedented “tie-point” free geolocation accuracy for a spaceborne SAR sensor. Here we describe how the accuracy was measured, and how it was achieved.

##### 4.5.1. Relative Localisation Accuracy

Given the broad range of focussed ASAR products produced by the PF-ASAR processor (see Table 3), it is important to ensure that all are geometrically consistent with one another. Comparisons between product categories produced using data from the same acquisition IMS/IMP/IMM/IMG, APS/APP/APM/APG, and WSS/WSM were made by ellipsoid-geocoding each product into a common geometry (for IM and AP the IMG/APG geometry was taken as the reference). Image matching between the resulting geocoded-ellipsoid-geocoded (GEC) images, followed by evaluation of relative shift statistics, showed geometric consistency

much smaller than the resolution of a single sample [18][19]. Small subswath-dependent residual shifts between WSS and WSM products were found to be less than 10% of a resolution cell. The confirmed high *relative* location accuracy gives one confidence to use only the highest resolution (SLC) products for *absolute* accuracy determination, and that the low level of location errors determined for those products is valid throughout the product tree. One may use the high resolution products as the primary calibration reference, and validate the remaining product categories “vicariously”.

##### 4.5.2. Absolute Geolocation Accuracy

During the ASAR mission, the absolute geolocation accuracy was monitored regularly using the ASAR transponders as targets. Solution of the Doppler and range equations using the transponder location and delay term together with the Envisat state vectors and image annotations provided a *predicted* location of the target in the image.

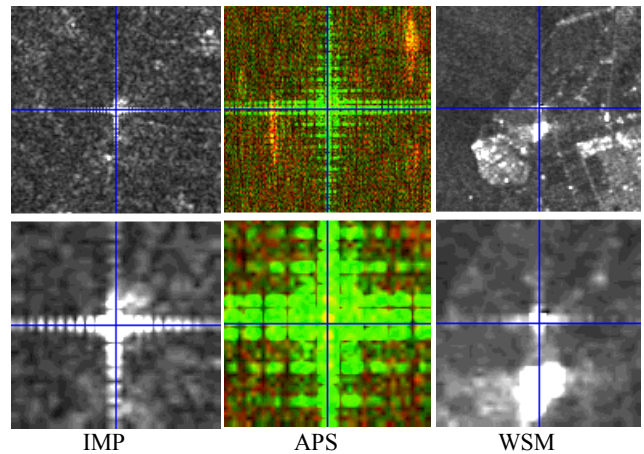


Figure 15. Netherlands transponder prediction (blue cross) vs. actual position in image (top: full product resolution, bottom: magnified view)

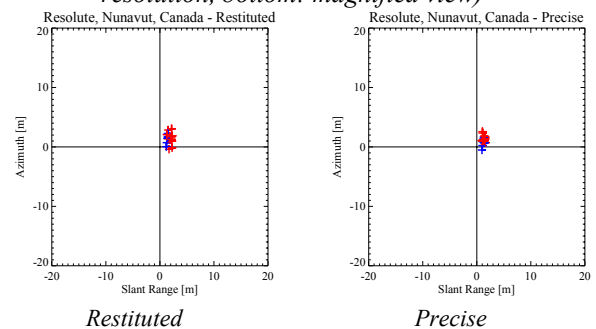


Figure 16. Resolute Radarsat transponder location prediction accuracy vs. state vector source

After confirmation that the strongest target in the neighbourhood of the prediction was the transponder, the image location was *measured* using zero padding and FFT interpolation, enabling a measurement

precision of 0.02 samples. Differences between predictions and measurements were tabulated and plotted for multiple geolocation methods, using a variety of state vector product qualities. Examples of such difference measurements are shown for the Radarsat transponder in Resolute, Canada above (Figure 16). On the left, predictions were based on restituted state vectors, on the right; one sees that slightly better accuracy was achieved using DORIS precise state vectors. Both results are a great improvement upon any preceding spaceborne SAR mission. For many applications, the restituted orbit quality is sufficient.

The timing of the ASAR receive window was calibrated in 2003 by observing differences between ascending vs. descending passes of such transponder measurements. The initial sampling window start time (SWST) bias value of  $3.2775 \times 10^{-7}$ s was replaced with an updated value of  $5.0995 \times 10^{-7}$ s, and made available in an updated ASA\_INS\_AX file for all interested in processing ASAR data [20]. All products generated by PF-ASAR after 13 December 2003 used the latter value. It is the date of processing that is pertinent, not that of the actual data acquisition.

A further processing artefact of note for PF-ASAR products is the so-called “bistatic” shift caused by the azimuth zero Doppler time (ZDT) annotation not being corrected for the “fast time” elapsing between echo reception and the real ZDT during the azimuth focussing operation. The geolocation grid annotated in all ASAR level 1 products is affected by this bias as is the ellipsoid-geocoding algorithm employed during IMG/APG product generation. For range-Doppler geocoding software however, the issue is strictly a slightly different annotation convention, and can be compensated within the geolocation procedure by adding an extra step to the azimuth index calculation [21]. If the effect is not compensated, then a range-dependent azimuth bias of  $\sim 20$ m is introduced, but no measurable residual effect has been detected if the standard correction described in [21] and [22] is applied.

Given a large set of differences calculated between predicted vs. measured image locations, the absolute location error (ALE) was estimated as the square root of the sum of the squares of the range and azimuth differences expressed in metres. With the exception of products subject to an intermittent range bias that were at the time being investigated with MDA Corporation, transponder measurements from Resolute (Canada) and the Netherlands made from 2003 to 2008 consistently showed ALE less than 10m, usually far lower [19]. Similar accuracies were measured using transponder images acquired after the ENVISAT orbit change in 2010 [23]. The intermittent range bias was later corrected in a PF-ASAR software upgrade by MDA.

Measurements made since the transponder redeployment indicated that the largest contributing error source appeared to be the quality of the transponder’s GNSS survey. If higher quality surveys of the transponder positions could have been made available, then improved ALE values would almost certainly have resulted. It is a testament to the quality of the ASAR instrument and processor that geolocation accuracy determination was more severely limited by the quality of the available ground surveys than by the instrument / processor themselves.

#### 4.6. Instrument Performance Verification

The SAR quality imagery is essentially based on analysis of the system response of two particular types of targets:

- Point targets such as transponders, used to assess the impulse response function of the system that is characterised by the 3dB spatial resolution and sidelobe characteristics.
- Distributed targets to assess the radiometric properties of the system using the statistical distribution of the pixel intensity.

Table 9 shows the Impulse Response Function (IRF) characteristics obtained from the transponder analysis during the ASAR mission for both high-rate and medium resolution products (ISLR, PSLR and SSLR are the integrated, peak and spurious sidelobe ratios respectively). All parameters are well within the requirements except for the APS product sidelobe ratios due to the IRF modulation caused by the discontinuity of the Doppler spectrum inherent to the ScanSAR imaging mode [24].

Table 9(a). HR IRF Characteristics

Product Type	Azimuth Res (m)	Range Res (m)	ISLR (dB)	PSLR (dB)	SSLR (dB)
IMP	22.12±0.48		-13.49±0.51	-16.66±0.97	-22.70±1.73
IMG	22.34±0.47	21.6 – 35.8	-13.57±0.50	-16.83±0.96	-23.45±1.68
IMS	4.77±0.03 5.56±0.06	9.43±0.05	-14.44±0.29	-18.97±0.40	-28.39±0.60
APP	27.45±0.80		-12.90±0.52	-19.06±0.93	-27.11±1.56
APG	27.49±0.77	22.6 – 36.4	-12.99±0.52	-19.14±0.91	-27.66±1.28
APS	4.29±1.77	8.39±0.06	4.04±2.41	-1.97±1.31	-16.45±4.23

Table 9(b). MR IRF Characteristics

Product Type	Azimuth Res (m)	Range Res (m)	ISLR (dB)	PSLR (dB)	SSLR (dB)
IMM	146.61±3.52	132.88±5.79	-7.37±4.4	-16.19±1.89	-16.18±4.62
APM	141.96±5.04	130.81±6.08	-9.30±4.59	-15.79±1.79	-17.65±4.42
WSM	114.39±5.79	124.78±8.84	-7.91±5.22	-12.38±2.02	-14.04±4.36

For the ground range detected products, the range resolution varies with incident angle. Figure 17 shows the measured range resolution for IMP and APP products. An excellent agreement is observed, with results well below the requirement of 30m at mid-range.

The pixel spacing of the IMP products is 12.5m causing them to be slightly under-sampled depending on the swath and the position within the swath [25].

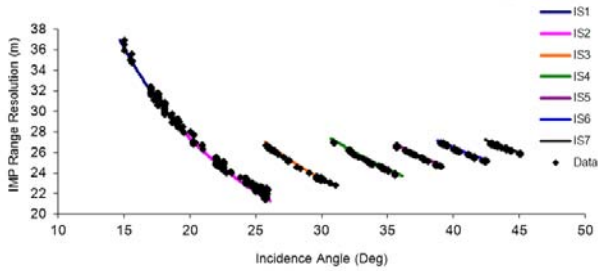


Figure 17(a) ASAR IMP range resolution measurements. Solid line is theoretical curve.

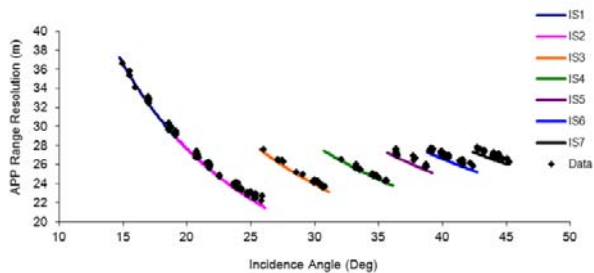


Figure 17(b) ASAR APP range resolution measurements. Solid line is theoretical curve.

Figure 18 provides the measured range resolution for one of the medium resolution products (WSM). The range resolution requirement for these products was 150m at mid-range. The pixel spacing for the MR products is 75m. Therefore most of the products do not respect the Nyquist criterion (i.e. the pixel size should be equal to or less than half the spatial resolution). In practice, systematic analysis of the data has demonstrated that it is not a problem except in the far swath portions and for the higher incident angle swaths, where the under sampling tends to bias the IRF response.

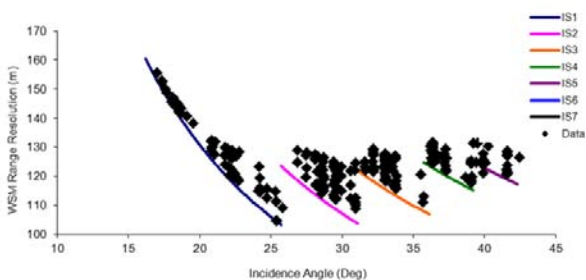


Figure 18. ASAR WSM range resolution measurements.

In addition to the IRF measurement, distributed targets of homogeneous backscatter were used to assess the radiometric accuracy and stability of the system. Table 10 presents the results in terms of Equivalent Number of Looks (ENL), giving an indication of the Radiometric Resolution. These values compare well with the

theoretical values for each product type based on the processing parameters such as look bandwidth and number of processed looks.

Table 10. Equivalent Number of Looks (ENL)

	IMP	IMS	IMM	APP	APS	APM	WSM
SS1	-	-	-	-	-	-	13.2
IS1	3.95	0.96	35.7	1.76	0.93	44.0	-
IS2	3.95	0.96	42.2	1.73	0.93	52.5	-
IS3/SS2	3.95	0.96	52.6	2.25	0.93	65.7	13.2
IS4/SS3	3.95	0.96	60.8	2.66	0.93	75.7	13.8
IS5/SS4	3.95	0.96	65.8	3.30	0.93	83.2	13.8
IS6/SS5	3.95	0.96	72.7	3.78	0.93	90.2	13.4
IS7	3.95	0.96	75.8	3.73	0.93	95.9	-

Finally, the upper limit to the noise equivalent sigma nought ( $NE\sigma_0$ ) of an image is estimated by measuring the radar cross-section of low backscatter regions. These targets of opportunity are typically oceans and inland waters with very low wind speed conditions. The results can be seen in Figure 19 for HR data over different polarisations (pre orbit change). The solid curves represent the theoretical values (the upper and lower curves are for the satellite altitude extremes). The measurements are as expected or better. Post-orbit change  $NE\sigma_0$  estimates are slightly better than pre-orbit change due to reduced slant range and hence a better SNR.

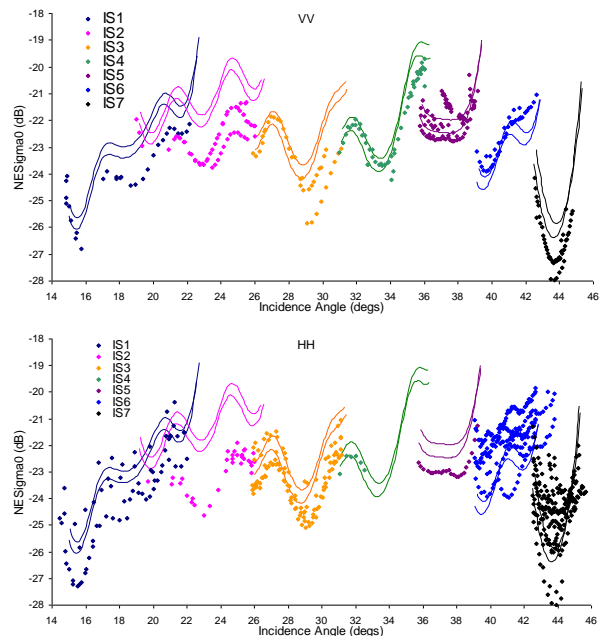


Figure 19. Noise equivalent sigma zero measurements for IM VV (top) and HH (bottom)

#### 4.7. Product Calibration

ASAR products (and all ESA SAR products up to now) are delivered in the radar brightness [26] (beta nought) convention. The conversion to beta, sigma, or gamma nought is left to the users or to dedicated tools. Calibration of ASAR products processed with the official ESA processor PF-ASAR is described in [24].

### 5. SPECIFIC SAR MISSIONS

#### 5.1. Wave Mission

Knowledge of ocean waves and wave climate is needed for various applications within offshore operations / engineering, fisheries, ship routing and coastal/harbour management. The measurement and analysis of directional ocean wave spectra have been a research topic for decades. Today, information on ocean wave spectra is provided by buoys, numerical models and HF radars. In the last decades, sea-surface remote sensing from satellites providing global measurements of ocean winds, wave height and wave spectra have become useful tools for both the oceanographic and the meteorological community. While scatterometers and altimeters are well proven and accepted techniques for measuring ocean surface winds and wave height, the use of SAR for measuring the directional wave (swell) spectra is still in its developing stage.

Nevertheless, since the launch of the ERS-1 satellite in 1991, global measurements of SAR ocean image spectra have been collected in the so-called Wave Mode (WM). The WM corresponds to small measurements called wave cells approximately 5 km along-track by (up to) 10 km across-track, acquired at 100 km intervals. The cells may have alternating positions in the swath or be in alternating swaths. The polarisation may also alter between VV and HH. However, the standard configuration is swath IS2 corresponding to an incident angle of  $22.7^\circ$  and VV polarisation.

With the launch of Envisat in 2002, a new era was initiated with the introduction of the WM Level 1 image cross-spectra product and the WM Level 2 wave spectra product. The Level 1 image spectrum is estimated by inter-looking of the complex imagedette followed by co- and cross-spectra estimation between the individual inter-look images. The Level 1 product is the input to the Level 2 processing, and allows retrieval of an ambiguity free estimate of the ocean swell spectra. The Level 2 product, consisting of the two-dimensional SAR ocean swell wave spectra, is provided in near real-time as part of the ESA Envisat ground segment processing. The WM Level 2 product has successfully been used in various applications such as swell tracking and assimilation in Numerical Weather Prediction (NWP) models [28].

The performance of the wave mode for swell wave spectra retrieval has been assessed using buoy and WAM data. Some key wave performance parameters [27] [29] [30] are listed in Table 11.

*Table 11. ASAR WM Level 2 Performance*

Wave Parameter	Bias	RMSE
Dominant Swell Wave Period [s]	0.1	1.7
Dominant Swell Wave Direction [°]	7	45
Swell Wave height [m]	0.1	0.4
Wind Speed [m/s]	0	1.8

#### 5.2. ASAR Polarimetric Mission

Polarimetric SAR missions are motivated by evidence that scattering from the Earth's surface is strongly dependent on the polarisation of the incident energy. As a consequence, polarimetric SAR data has been used for many applications in all fields of Earth remote sensing: forestry, agriculture, oceanography, snow and ice.

In general, a polarimetric SAR records the coherent (i.e. inter-channel phase preserving) and simultaneous illumination of the Earth's surface with different polarization states (e.g. H and V). This is usually achieved by using two separate transmit and receive chains for both polarisations. A dual-polarimetric mode has a conventional transmit PRF setup with two parallel receiving H/V modules. A fully-polarimetric mode, in addition, interleaves the transmission of H and V over the stream of pulses. The missions ALOS/PALSAR, Radarsat-2, TerraSAR-X and COSMO-SkyMED are indeed polarimetric missions, as they support operation in one or both of these modes.

##### 5.2.1. Alternating Polarisation

ASAR features multi-polarisation capability either in IM as it is able to transmit and receive at HH or VV and through the dedicated AP mode.

Similarly to classical dual-polarimetric mode, ASAR AP mode provides a pair of co-registered images with different polarisations in co-polarisation (HH/VV) or in cross-polarisation (HH/HV or VV/VH). However, AP does not really fall into the category of dual-polarimetric mode because it does not preserve the phase between polarimetric channels (i.e. it is not coherent). This is due to the fact that AP was implemented in a ScanSAR fashion, i.e. transmitting burst sequences with alternated polarisations during the antenna synthesis. This yielded alternating looks of approximately one fourth of the integration time and a

reduced spatial resolution compared with IM data.

It follows that a polarimetric analysis of the scene characteristics can only be performed partially using the backscatter coefficients for the polarisation combination of the ASAR AP product. Using alternate polarisation data results still in an advantage with respect to the single polarisation case for the purpose of quantitative remote sensing [31][32].

### 5.2.2. AP swath reduction

Section 3.5 describes a problem experienced with AP mode since the beginning of the mission. This led to the suspension of AP IS5 acquisitions at the end of 2006 and to a significant reduction in the use of all other swaths in early 2007. In May 2009, a patch was uplinked on-board in order to overcome this anomaly, allowing resumption of AP operations. However, it was made at the expense of an AP mode swath reduction (see Table 5).

## 6. ERS AND ASAR: TWO INSTRUMENTS ONE MISSION

One of the ASAR mission goals is to ensure continuity with the ERS mission. ESA implemented this requirement in three major ways.

First was provision of measurement continuity by acquiring the majority of IM and WV data in ERS-like mode. Second was harmonisation of the processors and formats. Indeed, the historical ERS processor (called VMP) was replaced in 2005 by the PF-ERS processor which is identical to PF-ASAR. PF-ERS allows ERS data to be processed with the same algorithm as ASAR, providing data in either CEOS or Envisat format. Third was the reprocessing of the ERS SAR mission. For the ERS IM mode, the scope was to reprocess the ERS data acquired in Zero Gyro Mode (ZGM) in order to derive reliable Doppler information to support the interferometric mission. For the WV mode, it consisted of reprocessing the entire ERS-1/2 WV mission using the same algorithm as ASAR in order to provide the scientific community with 20 years of homogeneous dataset in quality and format. This enables studies over a long term of the mechanisms of the ocean so important for climatology and meteorology.

## 7. SUMMARY

After an introduction of the ASAR instrument and products, this paper described the main events and performance results that occurred for the ASAR instrument during the just over 10 years of the Envisat mission. The ASAR mission provided an enhanced set of operating modes and product types compared to the ERS SARs as well as the operation and maintenance of an active antenna.

The quality assessment and calibration of ASAR products was improved and enhanced throughout the mission. This required a constant involvement from ESA and partners and also a constant dialogue with the user community. An example of this was WS burst synchronisation where an improvement was made part way through the mission to increase the probability of generating an interferogram from complex WS data.

Note that this paper has not discussed another key activity of the ASAR mission: SAR processor maintenance and evolution. The MDA PF-ASAR processor has had a number of updates throughout the ASAR mission (e.g. to correct product anomalies) including the generation of new product types (e.g. complex wide swath) and new algorithms (e.g. noise removal).

## REFERENCES

- [1] Envisat-1 Programme Proposal, ESA/PB-EO(93)22, ESA document.
- [2] Zink, M., H. Jackson, 'ASAR External Characterisation', Proc. of the Envisat Calibration Review, 2002. (<http://envisat.esa.int/calval/proceedings/>).
- [3] Torres, R., 'ASAR Instrument Stability', Proceedings of the Envisat Calibration Review (<http://envisat.esa.int/calval/proceedings/>).
- [4] ASAR Product Specification, Envisat Product Specification, Volume 8, PO-RS-MDA-GS-2009, Issue4, Revision B.
- [5] Rosich, B., 2003, 'ERS-2 SAR & Envisat ASAR Instrument/Data Status', Proceedings of the Fringe Workshop, 1-5 December 2003, ESRIN, Frascati, Italy.
- [6] Rosich, B., A. Monti-Guarnieri, D. D'Aria, I. Navas, B. Duesmann, C. Cafforio, P. Guccione, S. Vazzana, O. Barois, O. Colin & E. Mathot, 'ASAR Wide Swath Mode Interferometry: Optimisation of the Scan Pattern Synchronisation', Proc. of Envisat Symposium, 23-27 April 2007, Montreux, Switzerland.
- [7] Goetz, C., Jackson, H., Rosich, B., Tranfaglia, M., Meadows, P., Canela, M., Lorza-Pitt, R., Laur, H., Viau, P., 2007, 'Global Redeployment of the ENVISAT ASAR Transponders for Around Orbit Calibration', Proc. of the Envisat Symposium, 23-27 April 2007, Montreux, Switzerland.
- [8] Rosich, B., Meadows, P.J, Monti-Guarnieri, A., D'Aria, D., Tranfaglia, M., Santuari, M. & Navas, I., 2007, 'Review of ASAR Performance and Product Quality Evolution', Proc. of the Envisat Symposium, 23-27 April 2007, Montreux, Switzerland.
- [9] Miranda, N., P. Meadows, A. Pilgrim, 2009, 'ASAR Alternating Polarisation Product Update', ESRIN Technical Note IDEAS-BAE-SOM-REP-0391.
- [10] 'Envisat Mission Extension Beyond 2010, Scenario Description', ESA Internal document, PE-RP-ESA-SA-205, Issue/Revision 1/0, 15/10/2007.



- [11] 'Envisat Mission Extension Beyond 2010, Expected Evolution of Payload Performance', ESA internal document, PE-RP-ESA-SA-213, 09/01/2008.
- [12] 'Envisat Mission Extension Beyond 2010, Impact on Product Quality and Overall Performance', ESA internal document, ENVI-SPPA-EOPG-TN-08-0002, 08/04/2008.
- [13] Jackson, H., I. Sinclair, and S. Tam, 'Envisat/ASAR Precision Transponders'. CEOS SAR Workshop, Toulouse, October 1999.
- [14] Rosich, B., J. Closa, 'The internal calibration strategy on the ASAR ground processor', CEOS SAR Workshop, Tokyo, April 2001.
- [15] Closa, J., 'Internal calibration processing and processor normalization', Proc. of the Envisat Calibration Review, 2002. (<http://envisat.esa.int/calval/proceedings/>).
- [16] ASAR Cyclic Reports, [http://earth.esrin.esa.it/pcs/envisat/asar/public\\_reports/](http://earth.esrin.esa.it/pcs/envisat/asar/public_reports/).
- [17] ASAR Auxiliary Data Files Online Repository, [http://earth.esa.int/services/auxiliary\\_data/asar/](http://earth.esa.int/services/auxiliary_data/asar/).
- [18] Small D., Schubert A., Rosich B, Meier E., 'Geometric and Radiometric Correction of ESA SAR Products', Proc. Envisat Symposium, Montreux, Switzerland, Apr. 23-27, 2007.
- [19] Schubert A., Small D., Miranda N., Meier E., 'ASAR Product Consistency and Geolocation Accuracy', Proc. CEOS SAR Workshop 2008, Oberpfaffenhofen, Germany, November 2008.
- [20] Small D., Rosich B., Meier E., Nüesch D., 'Geometric Calibration and Validation of ASAR Imagery', Proc. CEOS SAR Workshop 2004, Ulm, Germany, 27-28 May 2004.
- [21] Small D., Rosich B., Schubert A., Meier E., Nüesch D., 'Geometric Validation of Low and High-resolution ASAR Imagery', Proc. 2004 Envisat & ERS Symposium, Salzburg, Austria, 6-10 Sept. 2004 (ESA SP-572, April 2005).
- [22] Small D., Schubert A., 'Guide to ASAR Geocoding', RSL-ASAR-GC-AD, Technical Note, Issue 1.01, 30 April 2008, 36p.
- [23] Schubert, A. & Small, D., 2011. 'ASAR Geometric Calibration Verification (Mission Extension)', Technical Note, Ref: RSL-ASAR11-GC-ACC, Issue 1.0, Nov. 2011, Zürich, Switzerland.
- [24] Rosich, B., P.J. Meadows, A. Monti-Guarnieri, 'Envisat ASAR Product Calibration and Product Quality Status', Proc. CEOS SAR Workshop 2004, Ulm, Germany, 27-28 May 2004.
- [25] M. Santuari, P. Meadows, N. Miranda, A. Smith, 'The Impact of Product Sampling on IRF Properties', Proceedings of the CEOS SAR Workshop, 27-28 November 2008, Oberpfaffenhofen, Germany.
- [26] Raney, R.K. et al., 1994. 'A Plea for Radar Brightness'. In International Geoscience and Remote Sensing Symposium IGARSS. IEEE, pp. 1090–1092. Available at: [http://ieeexplore.ieee.org/xpls/abs\\_all.jsp?arnumber=399352](http://ieeexplore.ieee.org/xpls/abs_all.jsp?arnumber=399352) [doi: 10.1109/IGARSS.1994.399352].
- [27] Collard F., Arduin F., Chapron B., 'Monitoring and analysis of ocean swell fields from space: New methods for routine observations', Journal of Geophysical Research, Vol. 114, C07023, doi:10.1029/2008JC005215, 2009.
- [28] Lotfi, A., Lefevre M., Hauser D., Chapron B., Collard F., 'The impact of using the upgraded processing of ASAR Level 2 wave products in the assimilation system', Proceedings of the Envisat Symposium, Montreux, Switzerland, 23-27 April 2007.
- [29] Queuiffeulon, P., F. Arduin, B. Chapron, F. Collard, J.-M. Lefevre, and C. Skandrani, 'Assessment and Improvement of Wave Modelling at Global Scales, Using Buoy, Altimeter and SAR Measurements', Proceedings of the Envisat Symposium, Montreux, Switzerland, 23-27 April 2007.
- [30] Collard F., and H. Johnsen, Comparison of Reprocessed ASAR WM Ocean Wave Spectra with WAM and Buoy Spectra, and Demonstration of Swell Tracking using WM, Envisat Symposium, Montreux, Switzerland, 23-27 April, 2007
- [31] Inglada J., Souyris J.-C., Henry C., Tison C., Incoherent SAR Polarimetric Analysis over Point Targets, IEEE Geoscience and Remote Sensing Letters, vol. 3, no. 2, April 2006.
- [32] Johnsen H., Engen G., Guitton G., 'Sea-surface polarization ratio from Envisat ASAR AP Data and comparison with models', Proceedings of the Envisat Symposium 2007, Montreux, Switzerland, 23–27 April 2007.